Modelling transverse gusts using pitching, plunging and surging airfoil motions

Jordan M. Leung * and Jaime G. Wong .†
Queen's University, Kingston, Ontario, K7L 3N6, Canada

Gabriel D. Weymouth ‡
University of Southampton, Southampton, England, SO17 1BJ, United Kingdom

David E. Rival §
Queen's University, Kingston, Ontario, K7L 3N6, Canada

Three model-motions were developed to replicate the aerodynamic response of a transverse gust. These motions included a pure-plunging and two three degree-of-freedom motions that approximated the angle-of-attack distribution produced by the gust. Using inviscid models and viscous flow simulations, the response of the gust and model-motions were compared as a function of the non-dimensional reduced frequency. The inviscid model was found to overestimate the influence of the rotational added-mass in the three degree-of-freedom motions. In contrast, the viscous flow simulations showed that the two primary sources of discrepancy between the gust and model-motions lie in the non-linear angle-of-attack distribution caused by the gust, and the wake development during the model-motions. Flow simulations showed that all three motions experienced greater than 90% agreement in lift for gusts with reduced frequencies less than 0.5, indicating that under this reduced frequency: 1) the effect of the gust convection is minimal; and 2) a pure-plunging motion may suffice for modelling gusts. However, at higher reduced frequencies the pure-plunging motion experiences greater than 10% worse agreement than the three degree-of-freedom motions. Overall, the motions provide a good approximation with greater than 90% accuracy in lift for gusts of reduced frequencies less than k = 0.75.

Nomenclature

b = model semi-chord

c = model chord

C_d = 2D drag coefficient

*Undergraduate Researcher, Department of Mechanical and Materials Engineering
†Postdoctoral Researcher, Department of Mechanical and Materials Engineering
‡Associate Professor, Marine and Maritime Institute
§Associate Professor, Department of Mechanical and Materials Engineering

C_l	=	2D lift coefficient
C_m	=	2D moment coefficient
k	=	reduced frequency
R^2	=	coefficient of determination
Re	=	chord-based Reynold's number
s	=	non-dimensional convective time
t	=	time, s
T	=	gust period, s
U_∞	=	free-stream velocity, m/s
$v(x')$	=	y'-component of relative flow velocity at a location x', m/s
v_g	=	gust profile, m/s
w_0	=	gust amplitude in terms of velocity, m/s
(x, y)	=	coordinate system in global frame, m
(x', y')	=	coordinate system in body-fixed frame, m
α	=	angle of attack, rad
α_0	=	gust amplitude in terms of angle of attack, rad
λ	=	gust wavelength, m
σ	=	dummy variable of integration
ϕ	=	pitch angle, rad
$\phi(s)$	=	Wagner function
τ	=	time delay due to gust convection, s
$\psi(s)$	=	Küsser Function
ω	=	gust angular frequency, rad/s

Subscripts and Superscripts

AM	=	added-mass
circ	=	circulatory
eff	=	effective
LE	=	leading-edge
TE	=	trailing-edge
$\dot{x}$	=	derivative of quantity x with respect to time

I. Introduction

Wind turbines, unmanned and micro aerial vehicles (UAVs and MAVs), and natural flyers all operate in gusty conditions. Smaller aircraft such as UAVs and MAVs are particularly susceptible to loss of stability due to gust response since the gust loadings are proportionally much higher relative to the wing loading of these small aircraft. A major goal of current research is to adequately model gusts for the purpose of active flow control, as shown in the work by Kerstens et al. [1]. Some classical methods of modelling gusts involve defining a gust as a random process, where the gusts that are defined in such a way are referred to as continuous gusts. This method of gust definition uses statistical methods, such as the models developed by von Kármán and Sears [2] and Liepmann [3]. These methods are used to model stochastic processes such as atmospheric turbulence. However, gusts with deterministic forms, known as discrete gusts, are also of major interest in aeronautics as these correspond to non-random effects with potentially large gust amplitudes. Certain classical models can predict the response of thin airfoils to discrete gusts and airfoil motions such as the indicial response methods of Küssner [4] and Wagner [5], and the frequency domain model of Theodorsen [6].

Experimental studies have been performed to understand the effect of discrete gusts in realistic flow conditions. However, producing a robust, highly-repeatable gust profile remains challenging. Rival et al. [7] and Hufstedler and McKeon [8] used oscillating wings upstream of a model to simulate a vortical gust. Kerstens et al. [1] used downstream shutters to oscillate the free-stream around a model. Perrotta and Jones [9] used a vertical jet in a water tunnel to produce a transverse gust. However, a method of replicating a gust by moving a model in a stationary flow field, instead of moving a fluid around a model, is desirable for many reasons. First, a method that involves moving a model in a stationary fluid can be more repeatable and reliable than allowing shed vortices to advect through a flow. Second, the complexity required to perform such a motion can be much lower than what is required to generate a gust through a moving-fluid.

Recently Fernando et al. [10] and Mulleners et al. [11] used surging motions to simulate a streamwise gust. In a streamwise gust, the differences between a moving-model and a moving-fluid case can be resolved by adding/subtracting buoyancy and added-mass forces as done by Granlund et al. [12]. However, to-date there has been limited success in developing such a method to model a traverse gust. In a transverse gust, the changes in aerodynamic forces arise due to a change in the effective angle-of-attack, which has been shown in past studies to be challenging to reproduce using a moving-model. Wong et al. [13] observed a discrepancy in force history when using a combined plunging-surging motion to replicate a transverse gust, as the convective speed of the gust front was found to vary the topology of the trailing-edge vorticity. Perrotta and Jones [9] used a plunging motion to model a transverse gust and observed unexpected wake dynamics during the gust recovery, indicating that the vortex dynamics involved must be adequately modelled to obtain an agreement in force history. Kriegseis et al. [14] showed the importance of the effective velocity history at the leading-edge during flat-plate model-motions, as it dictates vortex growth and overall force histories.

Since there is a clear need to have an experimental approach to model transverse gusts, the motivation in this study

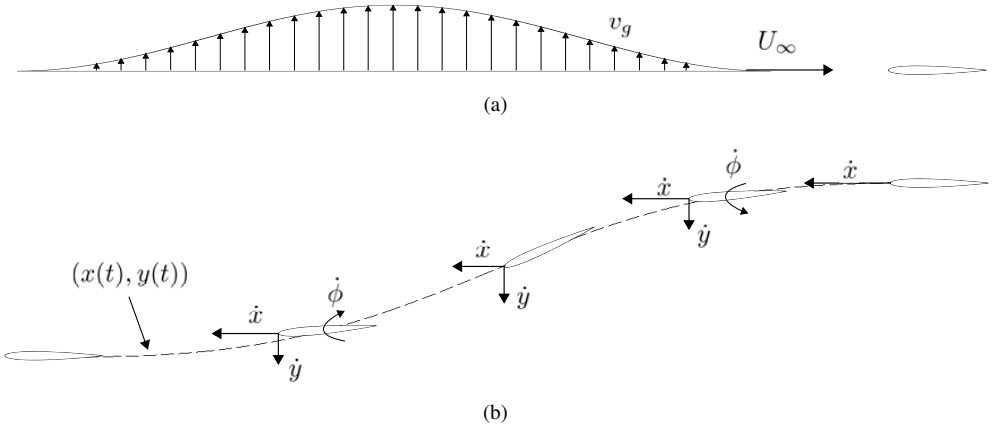

Fig. 1 A comparison of (a) a transverse gust convecting past an airfoil, and (b) a gust-replicating 3-DoF motion. In (a), the airfoil experiences a non-linear velocity distribution due to the gust convection, which is approximately replicated using the motion in (b).

was to first compare inviscid (conventional) modelling tools, similar to Baik et al. [15] and Granlund et al. [12], and then to examine more carefully with viscous simulations. To that end, three motions are investigated to build on the existing work in moving-model transverse gust simulation. The aerodynamic response of each motion is investigated as a function of reduced frequency under pseudo two-dimensional conditions. Future studies will need to consider additional effects such as fully-developed turbulent flow and finite aspect ratio lifting surfaces. In section II a generic transverse gust is defined and the development of the gust-replicating motions is discussed. Afterwards, both the inviscid and viscous methods used to evaluate the response of the gust and model-motions are described in section III. The aerodynamic responses obtained using these methods are presented and compared in section IV, and the conclusions drawn about their respective strengths and weaknesses are discussed in section V.

II. Background

Figure 1 shows a comparison of a generic gust and an exemplary three degree-of-freedom (3-DoF) gust-replicating motion used in this study. As a result of the convective velocity of the gust, the effective angle-of-attack at every location along the chord is delayed relative to the leading-edge. This delay creates a non-linear distribution of angle-of-attack along the chord of the model. A definition of the generic gust and the corresponding model-motions is described in detail in the following subsections.

A. Generic transverse gust

A *one-minus-cosine* transverse gust v_g is used in this study and is defined as:

$$v_{\mathrm{g}} = \begin{cases} 0 & t \leq 0 \\ \frac{w_0}{2}\left(1 - \cos\left(\frac{U_\infty k t}{b}\right)\right) & 0 < t \leq T \\ 0 & t > T \end{cases}, \tag{1}$$

where w_0 represents the gust amplitude, b the semi-chord of the profile experiencing the gust, $k = \omega b / U_\infty$ is the reduced frequency, and ω is the angular frequency. The reduced frequency is also related to the gust wavelength λ by $k = \pi c / \lambda$, where c is the chord. This particular gust form is consistent with the definition of a one-minus-cosine gust set by the US Federal Aviation Administration [16]. The time $t = 0$ corresponds to the moment where the gust front first impacts the leading-edge of the model. The gust is assumed to be frozen and convect at the free-stream velocity U_∞. As a result of the gust convection, the effective angle-of-attack at the trailing-edge is delayed relative to the leading-edge by a time $\tau = c/U_\infty$, as seen in equations 2 and 3:

$$\alpha_{\mathrm{eff}}^{\mathrm{LE}} = \begin{cases} 0 & t \leq 0 \\ \arctan\left(\frac{w_0}{2U_\infty}\left(1 - \cos\left(\frac{U_\infty k t}{b}\right)\right)\right) & 0 < t \leq T \\ 0 & t > T \end{cases}, \quad \text{and} \tag{2}$$

$$\alpha_{\mathrm{eff}}^{\mathrm{TE}} = \begin{cases} 0 & t \leq \tau \\ \arctan\left(\frac{w_0}{2U_\infty}\left(1 - \cos\left(\frac{U_\infty k (t-\tau)}{b}\right)\right)\right) & \tau < t \leq (T+\tau) \\ 0 & t > (T+\tau) \end{cases}. \tag{3}$$

For discussion purposes, the gust amplitude can also be defined in terms of an effective angle-of-attack amplitude $\alpha_0 = \arctan(w_0/U_\infty)$.

The reduced frequency can be related to the size of τ relative to the period T, or the chord length relative to the gust wavelength as $k/\pi = \tau/T = c/\lambda$. As large reduced frequencies represent time delays that are larger fractions of the overall motion, it is expected that there exists an upper-bound to the range of reduced frequencies that can be captured in a limited degree-of-freedom motion. The following subsection describes the development of three separate motions used to replicate the response of this gust.

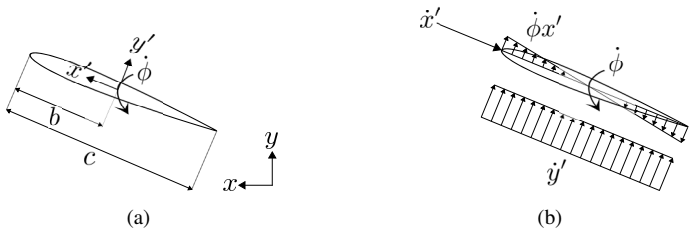

Fig. 2 A visualization of the 3-DoF kinematics, where: (a) shows the body-fixed coordinate system described by (x', y'), and (b) demonstrates how the relative flow velocity vectors are produced in the body-fixed frame.

B. Gust replicating motions

For the motions used to replicate the gust, a body-fixed frame of reference is defined with the origin $O_{x',y'}$ fixed to the centre-chord position, as shown in figure 2. The coordinates x' and y' are defined to be parallel and perpendicular to the chord line, respectively. At a position along the chord $(x', 0)$, the velocity due to a 3-DoF motion in the body-fixed coordinate system is given by:

$$\begin{bmatrix} \dot{x}' \\ \dot{y}' \end{bmatrix} = \begin{bmatrix} \cos\phi & -\sin\phi \\ \sin\phi & \cos\phi \end{bmatrix} \begin{bmatrix} \dot{x} \\ \dot{y} \end{bmatrix} + \dot{\phi} \begin{bmatrix} 0 \\ x' \end{bmatrix}, \tag{4}$$

where $\dot{x}$ and $\dot{y}$ are the velocities in the global coordinate system and $\dot{\phi}$ is the pitch rate. The direction of lift is defined to be parallel to y', such that the effective angle-of-attack is only dependent on the velocities in the body-fixed coordinate system:

$$\alpha_{\text{eff}} = \arctan\left(\frac{\dot{y}'}{\dot{x}'}\right). \tag{5}$$

To replicate the response of the gust, three gust-replicating motions were developed and investigated. The first *pure-plunging* motion matches the effective angle-of-attack history produced by the gust at the centre-chord location by plunging the model. The centre-chord is chosen as it is found to provide the best agreement with the gust response. A similar method was employed by Wong et al. [13], where the plunging response was delayed by a quarter-chord distance. Second, the 3-DoF *edge-matched* motion matches the effective angle-of-attack and velocity at both the leading and trailing-edge. Third, the 3-DoF *centre-matched* motion matches the effective angle-of-attack, velocity, and their gradients at the centre-chord. The differences between these three motions are visualized in figure 3. At higher reduced frequencies ($k = 0.75$) when the gust wavelength is the same order of magnitude as the chord, the differences in angle-of-attack gradient between each motion are substantial. The pure-plunging motion does not resolve the angle-of-attack distribution well, while the two 3-DoF motions tend to overestimate and underestimate the average angle-of-attack during certain phases of the motion. A detailed formulation of the two 3-DoF motions is provided in the following subsections.

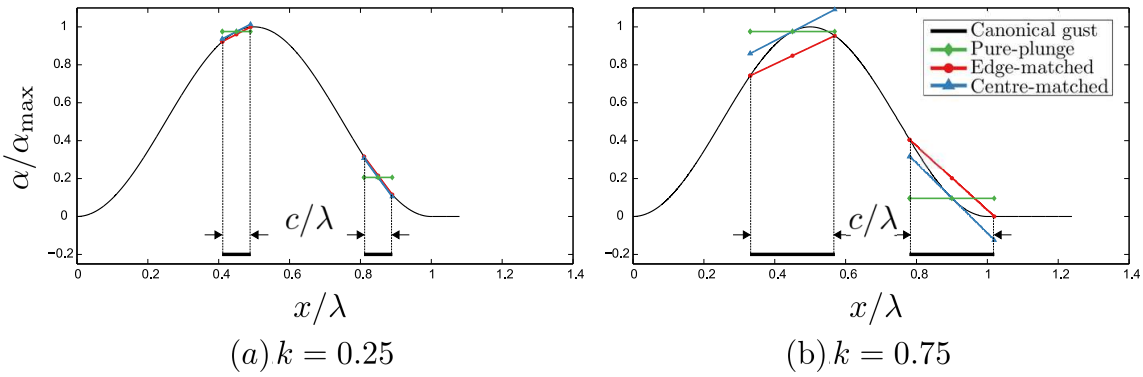

(a) $k = 0.25$ (b) $k = 0.75$

Fig. 3 A depiction of how each of the three motions differ in terms of the angle-of-attack distribution. For low reduced frequencies ($k = 0.25$) the difference between the motions is minimal, but at higher reduced frequencies ($k = 0.75$) the difference becomes considerable.

1. Edge-matched motion

For the edge-matched motion, the pitch rate is used to resolve the difference in the y' component of velocity between the leading and trailing-edge:

$$\dot{\phi} = \frac{v(b) - v(-b)}{c}, \tag{6}$$

where $v(b)$ and $v(-b)$ refer to the vertical component of velocity at the leading and trailing-edge produced by the gust. The x' component of velocity is defined such that the model is travelling at U_∞ in the x' direction at all times:

$$\dot{x}' = U_\infty. \tag{7}$$

Meanwhile, the y' component of velocity at the centre-chord is defined as the average of the leading and trailing-edge gust velocities:

$$\dot{y}'(0) = \frac{v(b) + v(-b)}{2}. \tag{8}$$

The combined effect of $\dot{x}'$, $\dot{y}'$, and $\dot{\phi}$ ensures the effective angle-of-attack and velocity at the leading and trailing-edge is equivalent to what is produced by the gust. The velocities in the global coordinate system, $\dot{x}$ and $\dot{y}$, necessary to execute these dynamics, can be obtained by rearranging Eq. 4 and solving at the centre-chord position:

$$\begin{bmatrix} \dot{x} \\ \dot{y} \end{bmatrix} = \begin{bmatrix} \cos\phi & \sin\phi \\ -\sin\phi & \cos\phi \end{bmatrix} \begin{bmatrix} U_\infty \\ \frac{v(b)+v(-b)}{2} \end{bmatrix}. \tag{9}$$

As seen in figure 3, this motion overestimates the average angle-of-attack at the start and end of the motion, and underestimates it near the peak. Therefore, at higher reduced frequencies, it is expected that the response of the edge-matched motion will tend to overestimate the lift near the start and end of the motion, while underestimating the

lift near the peak when compared to the gust.

2. Centre-matched motion

The velocity $\dot{y}'$ is defined identically between the centre-matched and pure-plunging motions, such that the velocity produced by the gust at the centre-chord is matched:

$$\dot{y}'(0) = v(0) = \begin{cases} 0 & t \leq \frac{\tau}{2} \\ \frac{w_0}{2}\left(1 - \cos\left(\frac{U_\infty k(t-\frac{\tau}{2})}{b}\right)\right) & \frac{\tau}{2} < t \leq (T + \frac{\tau}{2}) \\ 0 & t > (T + \frac{\tau}{2}) \end{cases}, \tag{10}$$

where $v(0)$ represents the vertical velocity of the gust at the centre-chord, and $\tau/2$ corresponds to a half-chord distance in convective time. The pitching motion is defined such that it matches the gradient of velocity produced by the gust at the centre-chord:

$$\dot{\phi} = \frac{\partial v(0)}{\partial x}, \tag{11}$$

The definition of $\dot{x}'$ is identical to that of the edge-matched motion (Eq. 7). The global velocity components required to execute this motion can be solved in the same way as the edge-matched motion by using Eq. 4:

$$\begin{bmatrix} \dot{x} \\ \dot{y} \end{bmatrix} = \begin{bmatrix} \cos\phi & \sin\phi \\ -\sin\phi & \cos\phi \end{bmatrix} \begin{bmatrix} U_\infty \\ v(0) \end{bmatrix}. \tag{12}$$

From figure 3 it is seen that this motion underestimates the average angle-of-attack at the start and end of the motion, and overestimates it near the peak - the opposite effect to the edge-matched motion. Therefore, at higher reduced frequencies, it is expected that the response of the centre-matched motion will tend to overestimate the peak lift, while underestimating the lift at the start and end of the motion. In the following section, the methods used to evaluate the response of the gust and motions are described in detail.

III. Methods

Inviscid models and viscous flow simulations using a flat-plate model with a Reynolds number of $Re = 1000$ were used in this study. Reduced frequencies varying from $k = 0.25$ to $k = 1$ were explored since below this range the motion becomes increasingly steady and no new insight is gained. Above this range the motion has surpassed the upper limit of reduced frequency where good agreement is found. Gust amplitudes of $\alpha_0 = 15°$ and $\alpha_0 = 30°$ were used to ensure flow separation was observed.

The inviscid analysis is used to generate preliminary conclusions regarding the similarities of the gust and model-

motions. This analysis allows for an estimate of a reduced frequency range where the gust convection has a notable effect on the response, while also estimating the contribution of added-mass to the lift response. Subsequently, a viscous analysis using flow simulations is described, which allows for the gust and model-motions to be compared under more realistic flow conditions.

A. Inviscid analysis

The indicial methods described by Leishman [17] are used to evaluate the inviscid lift response of the gust and the model-motions. The gust response is evaluated in the method of Kússner [4]:

$$C_l = \frac{2\pi}{U_\infty}\left(v_g(0)\psi(s) + \int_0^s \frac{dv_g(\sigma)}{ds}\psi(s-\sigma)d\sigma\right), \tag{13}$$

where $\psi(s) \approx 1 - 0.5e^{-0.13s} - 0.5e^{-s}$ is the Küssner function, $s = U_\infty t/b$ is a non-dimensional time expressed in semi-chords travelled, and σ is a dummy variable of integration. Similar, the circulatory lift response due to an arbitrary variation in angle-of-attack can be evaluated in the method of Wagner [5]:

$$C_l^{\text{circ}} = 2\pi\left(\alpha_{3/4}(0)\phi(s) + \int_0^s \frac{d\alpha}{ds}\phi(s-\sigma)d\sigma\right), \tag{14}$$

where $\phi(s) \approx 1.0 - 0.165e^{-0.0455s} - 0.335e^{-0.3s}$ is the Wagner function and $\alpha_{3/4}$ represents the effective angle-of-attack at the 3/4-chord location. Unlike the Küssner function, the Wagner function only includes the circulatory lift. Thus, the added-mass is evaluated in the method of Theodorsen [6] and Greenberg [18], such that for a 3-DoF motion with a pitch location at the centre-chord position the added-mass is given by:

$$C_l^{\text{AM}} = \frac{\pi b}{U_\infty}\left(\ddot{y}' + \dot{x}'\dot{\phi}\right), \tag{15}$$

such that both the circulatory and added-mass forces are evaluated in the body-fixed coordinate system.

B. Viscous analysis

To check the effectiveness of the gust-replication motions, a series of viscous flow computational fluid dynamic simulations were performed. The software that was used is called LilyPad (see Ref. [19]) which solves the full two-dimensional Navier-Stokes equations by applying the Boundary Data Immersion Method (see Ref. [20]) to immerse the dynamic solid boundaries into the fluid domain. This method has been shown to give accurate results for a variety of unsteady airfoil problems closely related to the current work, including unsteady dynamics due to a perching maneuver, as shown by Polet et al. [21], and the performance of tandem flapping foils, as shown by Muscutt et al. [22].

A Cartesian grid is used, which avoids the difficulties associated with meshing moving boundary problems, and

allows a large parameter space to be investigated with relative ease. A rectangular plate with thickness $a = 0.02c$ was used in the simulations, with no-slip boundary conditions applied on the body surface. The chord-based Reynolds number was set to Re = 1000. The numerical domain extends from $(x, y) = (-4c, -10c)$ to $(10c, 10c)$ with the plate at the origin. Unique to this study was the issue of adding the convecting gust to the simulations. This was achieved by adjusting the initial conditions and boundary conditions in the numerical domain. The gust was defined uniformly by Eq. 1. All simulations were initiated $t/T = 2$ before the gust interacted with the plate and run until $t/T = 1$ after the gust had passed the plate.

A numerical convergence study was performed with $k = 0.5$ and $\alpha_0 = 15°$ for both the gust and centre-matched motion to determine the appropriate grid resolution for the parameter studies. Testing resolutions of $h/c = 1/32 - 1/180$ showed between second and third order convergence and that a resolution of $h/c = 1/90$ resulted in lift predictions with only 1.8% (gust) and 2.3% (centre-matched) error compared to simulations using twice as many points. This resolution was used for the remainder of the work.

IV. Results

In this section the results of the inviscid analysis are presented first, and preliminary conclusions drawn from this analysis are discussed. The viscous results are presented afterwards and the agreement between the response of the gust and model-motions under these conditions is examined.

A. Inviscid results

Figure 4 shows a comparison of the lift response of the gust and the various model-motions at $k = 0.25$ and $k = 0.75$. Differences in the response of each motion are only evident at higher reduced frequencies, where the motion responses experience a negative phase shift relative to the gust response. This shift can be explained due to the effect of added-mass shown in the bottom of figure 4. During the first half of the motion, the added-mass is positive and creates the appearance of a negative phase shift. Meanwhile, in the second half of the motion the added-mass is negative, also causing the appearance of a negative phase shift. The magnitude of this phase shift increases with reduced frequency. Thus, the inviscid model indicates that the relative contribution of added-mass to the total lift differs between the model-motions and the gust.

Figure 4 also shows how the agreement (quantified by linear regression R^2) in the lift response varies with reduced frequency. The agreement of each motion with the gust response drops rapidly at higher reduced frequencies, and tends towards $R^2 = 1$ as k tends towards 0. The inviscid analysis predicts the pure-plunging motion to perform the best at all reduced frequencies, which does not prove true in the viscous analysis when flow separation occurs. This difference between the models is a result of the inviscid model overestimating the influence of the rotational added-mass in the 3-DoF motions, an occurrence that is not observed in the viscous results that follow.

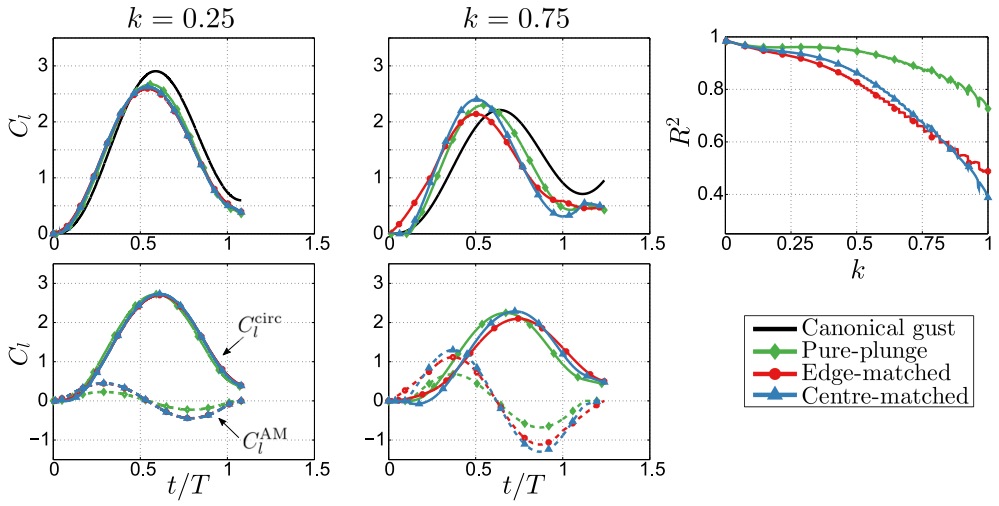

Fig. 4 A comparison of the inviscid lift response of the gust and model-motions (top) at $\alpha_0 = 30°$, and the breakdown of added-mass and circulatory forces in the model-motions (bottom). The agreement between the gust and motions quantified by R^2 is shown in the top-right.

B. Viscous results

A comparison of the lift, drag, and moment response of the gust and each model-motion under more realistic viscous flow conditions is shown in figure 5. The lift response of the gust is the primary area of interest as it drives effects such as dynamic stall. As such, the discussion presented revolves around the lift response, while the drag and moment response are used to gain additional insight into the flow physics. As a result of the non-linear angle-of-attack distribution produced by the gust, the accuracy of the lift response of the gust-replicating motions deteriorates with increased reduced frequency. The linear angle-of-attack distribution produced by the motions can only approximately replicate that of the gust, as such a noticeable drop in agreement is experienced above $k = 0.75$. The decline in agreement is clearly demonstrated in terms of R^2 as shown in figure 5 (a).

In general, the centre-matched motion most consistently replicates the gust response. In contrast, the edge-matched motion underestimates the peak lift at higher reduced frequencies as a result of underestimating the average angle-of-attack. Meanwhile, the pure-plunging motion performs particularly poorly at high reduced frequencies as a result of the lack of angle-of-attack gradient. This effect is reflected clearly in the significantly poorer prediction of the moment response. Since less than a 10% difference is seen in the lift histories of the gust and each model-motion at $k \leq 0.50$, it is concluded that the effect of the gust convection on the lift response is minimal at reduced frequencies under 0.50. As such, a pure-plunging motion may suffice for modelling transverse gusts of $k \leq 0.50$. However, the need for a 3-DoF motion is clear at higher reduced frequencies where the difference in accuracy between the pure-plunging and 3-DoF motions is significant.

In each of the test cases, the response of the gust and each motion display similar characteristics from $t = 0$ until the peak lift occurs, after which the behaviour during the recovery period differs between the gust and each motion. This

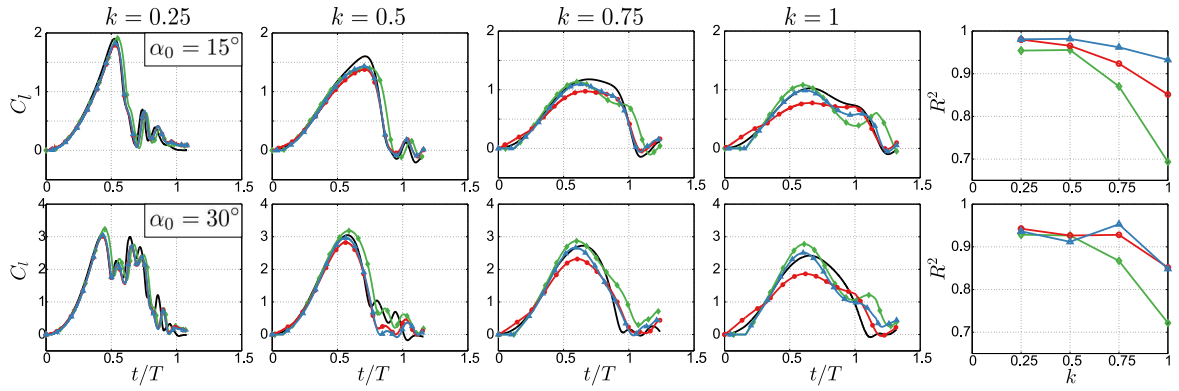

(a) C_l response

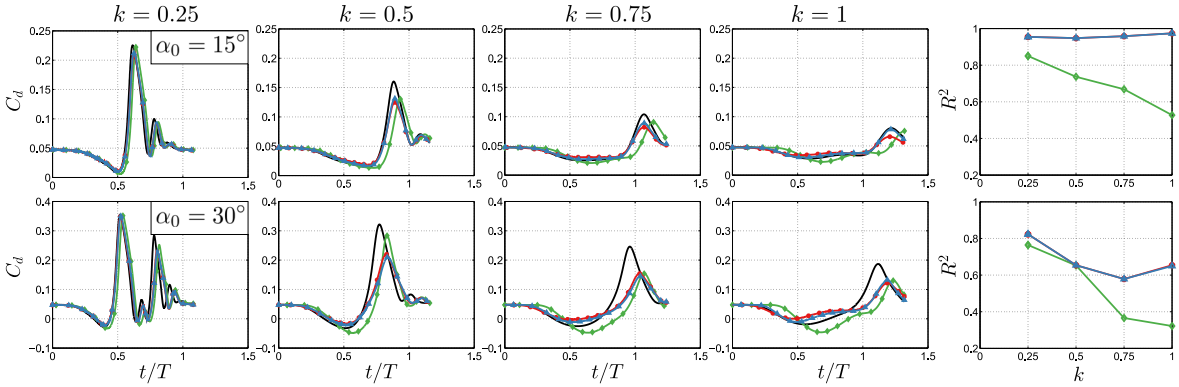

(b) C_d response

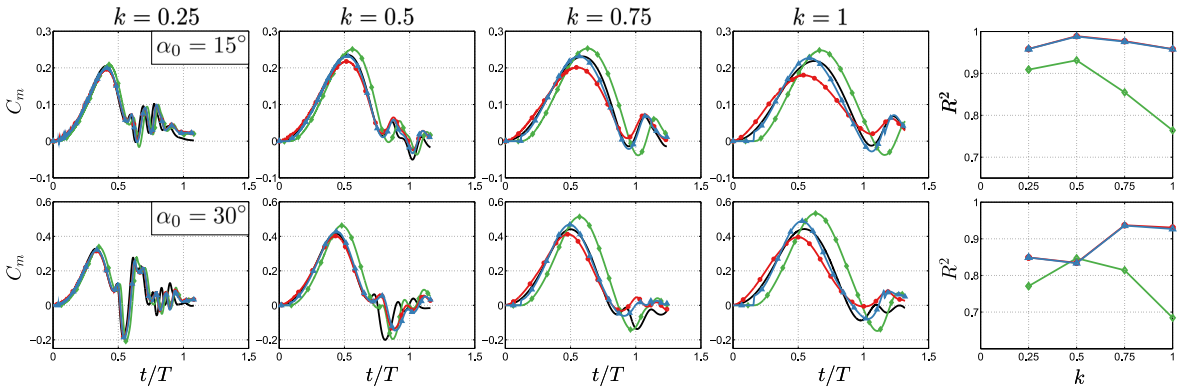

(c) C_m response

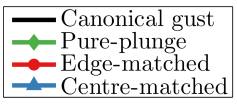

Fig. 5 A comparison of the lift (top), drag (middle), and moment (bottom) response obtained using viscous flow simulations for the gust and model-motions at $\alpha_0 = 15°$ and $\alpha_0 = 30°$. The agreement of each test case quantified by R^2 is shown on the far right.

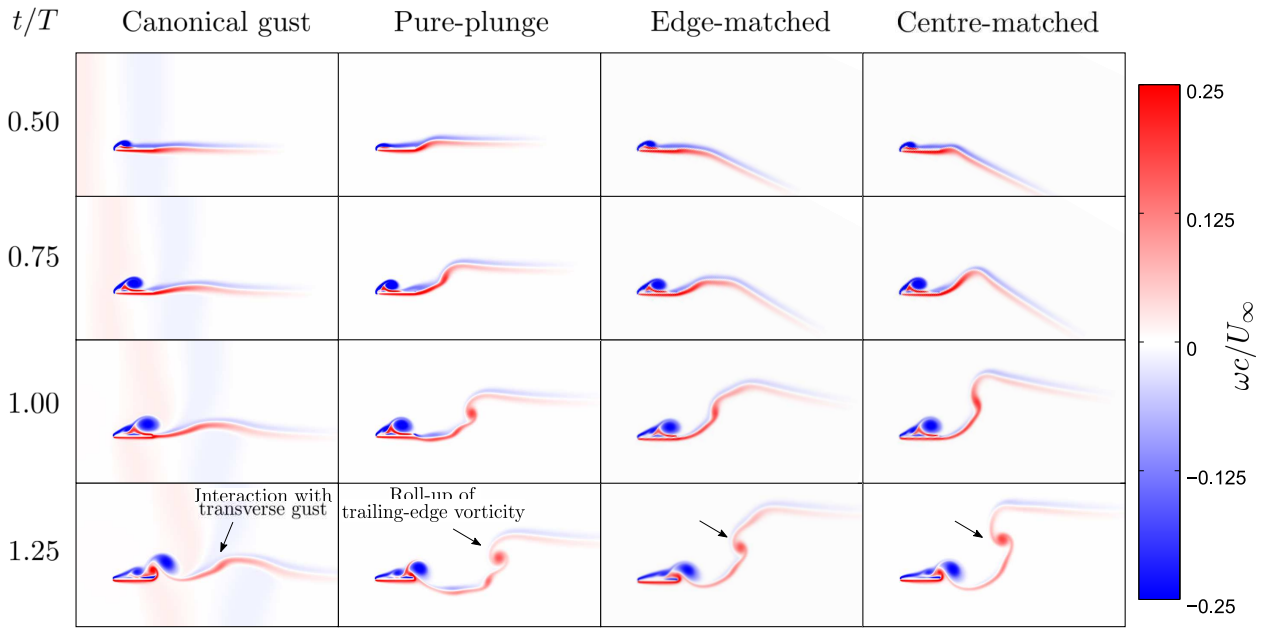

Fig. 6 A comparison of the flow fields at a reduced frequency of $k = 1.00$ and a gust amplitude of $\alpha_0 = 30°$. A difference in the downstream wake in the recovery period is seen, marked by the black arrows.

is especially noticeable in the drag response in the cases where $\alpha_0 = 30°$, as the motions have difficulty replicating the peak drag in the recovery period. This discrepancy is likely a consequence of the difference in wake development between the gust and the motions as shown figure 6. The vorticity in the transverse gust and the developing wake interact with each other; an effect not present in the model-motions. The vorticity cancellation in the case of the gust is missing in the motion cases, causing a more pronounced roll-up of trailing-edge vorticity due to the acceleration of the model relative to the downstream wake. A similar discrepancy in wake dynamics was also observed in Wong et al. [13].

V. Conclusions

In this study, the feasibility of replicating the lift response of a transverse gust using pitching, plunging, and surging motions was investigated. Three gust-replicating motions were considered: a pure-plunging motion and two 3-DoF motions that approximated the angle-of-attack distribution caused by the gust. Transverse gusts with one-minus-cosine profiles, reduced frequencies of $k = 0.25$ to $k = 1$, and amplitudes of $\alpha_0 = 15°$ and $\alpha_0 = 30°$ were analysed on a flat-plate model in inviscid conditions and at $Re = 1000$.

The inviscid model overestimated the influence of the rotational added-mass in the 3-DoF motions that was not present in the gust itself. However, the results of the viscous simulations showed that each motion exhibited similar agreement in lift history with $R^2 > 0.90$ for lower reduced frequencies of $k \leq 0.5$. From this agreement it was concluded that the effect of the gust convection on the lift response is minimal at $k \leq 0.50$, indicating that a pure-plunging motion could adequately simulate traverse gusts under at these frequencies. For $k > 0.50$, the agreement of the pure-plunging

model rapidly deteriorates and the centre-matched motion proves the most consistent in replicating the gust response. The two primary sources of discrepancy between the gust and the model-motions lie in the non-linear angle-of-attack distribution of the gust, and the wake development during the model-motions, which is likely due to the interaction of the vorticity in the transverse gust and the developing wake. This effect is not present in the model-motions. While the model-motions have difficulty replicating gusts on the order of $k = 1$, they provide an approximation with >90% accuracy in lift for gusts of $k \leq 0.75$.

References

[1] Kerstens, W., Pfeiffer, J., Williams, D., King, R., and Colonius, T., "Closed-Loop Control of Lift for Longitudinal Gust Suppression at Low Reynolds Numbers," *AIAA Journal*, Vol. 49, No. 8, 2011, pp. 1721–1728.

[2] von Kármán, T., "Progress in the statistical theory of turbulence," *Advances in Applied Mechanics*, Vol. 19, No. 12, 1948, pp. 793–800.

[3] Liepmann, H. W., "On the Application of Statistical Concepts to the Buffeting Problem," *Journal of Aeronautical Sciences*, Vol. 19, No. 12, 1952, pp. 793–800.

[4] Küssner, H. G., "Zusammenfassender Bericht über den instationären Auftrieb von Flügeln," *Luftfahrtforschung*, Vol. 13, No. 12, 1936, pp. 410–424.

[5] Wagner, H., "Über die Entstehung des dynamischen Auftriebes von Tragügeln," *Zeitschrift für Angewandte Mathematik und Mechanik*, Vol. 5, No. 1, 1925, pp. 17–35.

[6] Theodorsen, T., "General Theory of Aerodynamic Instability and the Mechanism of Flutter," *National Advisory Committee for Aeronautics*, 1935.

[7] Rival, D. E., Hass, G., and Tropea, C., "Recovery of Energy from Leading- and Trailing-Edge Vortices in Tandem-Airfoil Configurations," *Journal of Aircraft*, Vol. 48, No. 1, 2011.

[8] Hufstedler, E., and McKeon, B., "Isolated Gust Generation for the Investigation of Airfoil-Gust Interaction," *46th AIAA Fluid Dynamics Conference*, AIAA, Reston, VA, 2016.

[9] Perrotta, G. M., and Jones, A. R., "Transient aerodynamics of large transverse gusts and geometrically similar maneuvers," 54th AIAA Aerospace Sciences Meeting, AIAA SciTech Forum, 2016.

[10] Fernando, J. N., Marzanek, M., Bond, C., and Rival, D., "On the seperation mechanics of acceleration spheres," *Physics of Fluids*, Vol. 29, 2017.

[11] Mulleners, K., Mancini, P., and Jones, A. R., "Flow Development on a Flat-Plate Wing Subjected to a Streamwise Acceleration," *AIAA Journal*, Vol. 55, No. 6, 2017.

[12] Granlund, K., Monnier, B., Ol, M., and Williams, D., "Airfoil longitudinal gust response in separated vs. attached flows," *Physics of Fluids*, Vol. 26, 2014.

[13] Wong, J., Mohebbian, A., Kriegseis, J., and Rival, D., "Rapid flow seperation for transient inflow conditions versus accelerating bodies: An investigation into their equivalency," *Journal of Fluids and Structures*, Vol. 40, 2013, pp. 257–268.

[14] Kriegseis, J., Kinzel, M., and Rival, D. E., "On the persistence of memory: do initial conditions impact vortex formation?" *Journal of Fluid Mechanics*, Vol. 736, 2013.

[15] Baik, Y., Bernal, L., Granlund, K., and Ol, M., "Unsteady force generation and vortex dynamics of pitching and plunging aerofoils," *Journal of Fluid Mechanics*, Vol. 709, 2012, pp. 37–68.

[16] Federal Aviation Administration, "Advisory circular 25.341-1: Dynamic Gust Loads," , dec 2014.

[17] Leishman, J., *Principle of Helicopter Aerodynamics*, 2nd ed., Cambridge University Press, 2006.

[18] Greenberg, J. M., "Airfoil in Sinusoidal Motion In a Pulsating Stream," Technical Note 1326, National Advisory Committee for Aeronautics, jun 1947.

[19] Weymouth, G. D., Maertens, A., Izraelevitz, J., and Schulmeister, J., "Lily Pad: Real-time two-dimensional fluid/structure interaction simulations," *The Journal of Open Source Software*, 2111. URL `https://github.com/weymouth/lily-pad`.

[20] Maertens, A. P., and Weymouth, G., "Accurate Cartesian-grid simulations of near-body flows at intermediate Reynolds numbers," *Computer Methods in Applied Mechanics and Engineering*, Vol. 283, 2015, pp. 106–129. doi:https://doi.org/10.1016/j.cma.2014.09.007.

[21] Polet, D. T., Rival, D. E., and Weymouth, G. D., "Unsteady dynamics of rapid perching manoeuvres," *Journal of Fluid Mechanics*, Vol. 767, 2015, pp. 323–341. doi:10.1017/jfm.2015.61.

[22] Muscutt, L., Weymouth, G. D., and Ganipathisubramani, B., "Performance augmentation mechanism of in-line tandem flapping foils," *Journal of Fluid Mechanics*, Vol. 827, 2017. doi:https://doi.org/10.1017/jfm.2017.457.